Complex scaled spectrum completeness for coupled channels

B.G. Giraud, K. Kato, A. Ohnishi

Complex Scaled Spectrum Completeness for Coupled Channels

Article *in* Journal of Physics A General Physics · April 2005

DOI: 10.1088/0305-4470/37/48/004 · Source: arXiv

3 authors, including:

Akira Ohnishi
Kyoto University
272 PUBLICATIONS **3,078** CITATIONS

SEE PROFILE

Complex Scaled Spectrum Completeness for Coupled Channels

B.G. Giraud
giraud@spht.saclay.cea.fr, Service de Physique Théorique, DSM, CE Saclay, F-91191 Gif/Yvette, France

and

K. Katō and A. Ohnishi
kato@nucl.sci.hokudai.ac.jp, ohnishi@nucl.sci.hokudai.ac.jp, Division of Physics, Graduate School of Science, Hokkaido University, Sapporo 060-0810, Japan
(February 9, 2008)

The Complex Scaling Method (CSM) provides scattering wave functions which regularize resonances and suggest a resolution of the identity in terms of such resonances, completed by the bound states and a smoothed continuum. But, in the case of inelastic scattering with many channels, the existence of such a resolution under complex scaling is still debated. Taking advantage of results obtained earlier for the two channel case, this paper proposes a representation in which the convergence of a resolution of the identity can be more easily tested. The representation is valid for any finite number of coupled channels for inelastic scattering without rearrangement.

I. INTRODUCTION, NOTATIONS

As is well known, the CSM converts the description of resonances by non-integrable Gamow states into one by square integrable states while leaving the discrete spectrum unchanged [1]. Cuts describing the continuum are rotated, however, but this may be advantageous, since they are thus disentangled when their thresholds differ from one another. (We are not interested, in this paper, in the case of channels with identical thresholds.) It is then expected that the continuum corresponding to such rotated cuts makes a much smoother contribution to the calculation of collision amplitudes, level densities, strength functions and sum rules [2] [3], since narrow resonant processes have been assumed to be peeled out explicitly by the CSM. The CSM Hamiltonian, unfortunately, is not hermitian any more, and it is not obvious that a resolution of the identity in terms of its bound states, resonances and presumably damped continuum is possible. For the one channel case, convincing arguments have been advanced a long time ago [4] to prove that this resolution exists. More recently [5], a detailed investigation of the case of two channels, coupled by straightforward potentials, generated a contour integration of the usual Green's function which provided the identity resolution. The task was made reasonably easy by the small complication of the Riemann surface in that case. The purpose of the present paper is to capitalize on the methods used for that two channel case and attempt a generalization to any finite number of channels, despite the more complicated nature of the relevant Riemann surface. We shall assume, naturally, that there already exists, derived from single poles and usual cuts, a resolution of the identity for the initial Hamiltonian, before its modification by complex scaling. Our problematics would be meaningless otherwise.

Several earlier studies, in particular by [6] [7], have been concerned with a description of resonances with square integrable states, without complex scaling. They did not restrict to the consideration of just simple poles of the S-matrix and investigated how one might, as rigorously as possible, define initial wave packets for the description of decaying states; the non purely exponential nature of their decays received a detailed attention, via the analysis of their time dependent evolutions. The present paper, however, will be content with a Gamow definition of resonances, by means of simple poles; our aim is just to generate a resolution of the identity, with time independent states extending to asymptotic regions. For earlier searches of a complete basis of states, including resonances, but within a compact interaction volume, we may refer to the review by [8] of R-matrix methods and their extensions. See also [9] and in particular the comparison of "class B" and "class D" theories.

In this paper, we shall again assume that all potentials $V_{in}(r)$ driving the channels and their couplings are local and so short ranged, Gaussian-like for instance, that the $2N$ Jost solutions of the N coupled equation system,

$$-\psi''_{ij}(k_j,r)+\sum_{n=1}^{N}\left[e^{2i\theta}V_{in}(e^{i\theta}r)+\left(\frac{\ell_i(\ell_i+1)}{r^2}-k_i^2\right)\delta_{in}\right]\psi_{nj}(k_j,r)=0,\quad i,j=1,...,N, \tag{1}$$

exist and are analytical in the whole complex domain of all the momenta k_j. The radius r runs from 0 to $+\infty$, obviously, and the number N of channels is taken as finite. As an additional technicality we also assume, naturally, that the products $V_{in}\,\psi_{nj}$ do not diverge for $r \to 0$ when singular solutions of Eqs.(1) are considered.

We select the threshold of the lowest channel as the origin of the complex energy plane, hence $E \equiv k_1^2$. The other channels with their physical thresholds E_j^*, which are real and positive numbers, now define channel momenta according to, $E_j = k_j^2 = E - e^{2i\theta}E_j^*$. Notice that, given a real number E_j^* defining a physical threshold, the usual complex scaling where p^2 becomes $e^{-2i\theta}p^2$ and r becomes $e^{i\theta}r$ does not change E_j^* and rotates the corresponding cut by angle -2θ. But here, we have a slightly different representation, because the Hamiltonian has been multiplied by $e^{2i\theta}$. Hence kinetic operators in our Hamiltonian H, see Eqs.(1), are just $-d^2/dr^2$, every cut rotates back into being "horizontal"and starts from $e^{2i\theta}E^*$. For time dependent studies. it will make sense to scale time, conjugate of energy, by a factor $e^{-2i\theta}$. This will prevent those resonant wave packets, the energies of which have a positive imaginary part as eigenvalues of H, from exploding when $t \to +\infty$.

Also in this paper no rearrangement is allowed, channels are defined by just internal excitations of the projectile and/or the target, hence all reduced masses are equal. Finally we exclude from this paper the consideration of abnormal thresholds; we shall only discuss the case of "square root thresholds". This is generic enough.

It is understood here and from now on that a first subscript, such as i or n, denotes the component of each wave ψ in channel i or n, then that any superscript, $\pm$, or second subscript, j, denotes the boundary condition which defines ψ. For a Jost solution $f_{.j}^{\pm}$, the boundary condition that we choose is "asymptotic flux $e^{\pm i(k_j r - \ell_j \pi/2)}$ in channel j and no asymptotic flux in the other channels". It is well known that for $r \to 0$, the components of such Jost solutions are proportional to $(k_i r)^{-\ell_i}(2\ell_i - 1)!!$. For a regular solution $\varphi_{.j}$, the boundary condition that we choose sits at $r = 0$ and reads, "$\lim_{r\to 0}(k_i r)^{-\ell_i - 1}\,\varphi_{ij}(r) = 0\ \ \forall i \neq j$, while, for $i = j$, then $\lim_{r\to 0}(k_j r)^{-\ell_j - 1}\,\varphi_{jj}(r) = 1/(2\ell_j + 1)!!$.

Following Newton [10], it is convenient, given E and r, to set the column vectors $\varphi_{.j}$ into a matrix $\mathbf{\Phi}(E, r)$ of regular solutions and the Jost solutions $f_{.j}^{+}$ (resp. $f_{.j}^{-}$) into a similar matrix $\mathbf{f}^{+}(E, r)$ (resp. $\mathbf{f}^{-}$). It is also convenient to notice that $\mathbf{\Phi}$, viewed as a function of the k_j's as if these were independent momenta, is even under any reversal of a k_j into $-k_j$. Such is not the case for $\mathbf{f}^{+}$; analytic continuations in either energy or momenta planes can introduce one (or several) $f_{.j}^{-}$'s into $\mathbf{f}^{+}$.

For our oncoming argument we must use the Wronskian matrix with matrix elements the Wronskians $\mathcal{W}\,(f_{.m}^{+}, \varphi_{.n})$ of the Jost solutions $f_{.m}^{+}$ with the regular ones $\varphi_{.n}$. This, for s waves, is the transposed of $\mathbf{f}^{+}$ at $r = 0$,

$$\mathbf{W}(E) = \tilde{\mathbf{f}}^{+}(E, 0), \tag{2}$$

and for other angular momenta is only a slight modification of $\tilde{\mathbf{f}}^{+}(E, 0)$. (Rather than just $\tilde{\mathbf{f}}^{+}(E, 0)$ one must use limits of products $(k_i r)^{\ell_i} f_{ij}^{+}/(2\ell_i - 1)!!$ at $r = 0$, explicitly, but we will disregard this technicality.) The Green's function $\mathbf{G}$ is then found as,

$$\mathbf{G}(E, r, r') = \mathbf{\Phi}(E, r)\,[\mathbf{W}(E)]^{-1}\,\tilde{\mathbf{f}}^{+}(E, r') \ \text{ if } r < r', \quad \mathbf{G}(E, r, r') = \mathbf{f}^{+}(E, r)\,[\tilde{\mathbf{W}}(E)]^{-1}\,\tilde{\mathbf{\Phi}}(E, r') \ \text{ if } r > r'. \tag{3}$$

Here each tilde $\tilde{}$ means transposition; we refer to [10] or to Appendix A of [5] for the derivation of such formulae for $\mathbf{G}$. Despite different formulae whether $r > r'$ or $r < r'$, and the lack of hermiticity, $\mathbf{G}$ is symmetric, namely $\mathbf{G}(r, r') = \mathbf{G}(r', r)$.

It will be noticed that the CSM, as we describe it by the system of Eqs.(1), locates thresholds on a segment of the complex E plane with slope 2θ, extending from $E = 0$ to $e^{2i\theta}E_N^*$, and that the channel cuts are rotated back into being "horizontal". Conversely, bound states lie on a negative semiaxis rotated by 2θ and resonances are rotated by 2θ as well. This slight change of representation changes nothing to the physics, obviously. For trivial technical reasons [5], we normalize energy units so that $E_N^* = 4$. Also we shall use a short notation, $k \equiv k_1$ and $K \equiv k_N$. We show in Figure 1 the cut energy plane in an illustrative, four channel situation when $\theta = \pi/6$, $E_2^* = 1.5$ and $E_3^* = 3.5$.

Equipped with this slightly unwieldy formalism, we can now investigate whether there exists a representation, and an integration contour, such that the traditional integral, $\mathcal{I} = \int dE\,\mathbf{G}(E, r, r')$, calculated in two different ways, generates a resolution of the identity. This question of a representation and a contour is the subject of Section II, the main part of our argument. Additional considerations on the two ways of calculating this integral make the subject of Section III. A discussion and conclusion are proposed in Section IV.

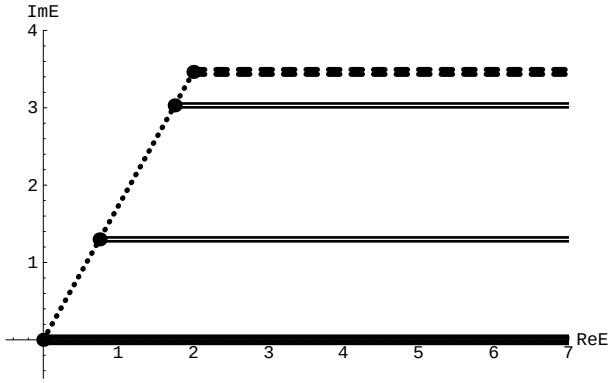

FIG. 1. E-plane. Physical cuts for a four channel case when $\theta = \pi/6$, $E_2^* = 1.5$, $E_3^* = 3.5$ and $E_4^* = 4$. Lowest channel, heavy full lines, highest channel, heavy dashed lines, intermediate channels, lighter full lines. The dotted segment with slope $\pi/3$ is the locus of thresholds (big dots) in this representation.

II. REPRESENTATIONS AND CONTOURS

A. Energy plane

From Fig. 1 it is intuitive that one could start, for instance, from $+\infty$ along the lower rim of the lowest channel cut, return to the origin, $E = 0$, proceed to $+\infty$ again on the upper rim, then join there the lower rim of the second cut, return to the threshold of this second cut, go to $e^{2i\theta}E_2^* + \infty$ along the upper rim, join the third cut lower rim at infinity, etc., until arriving at $e^{2i\theta}E_N^* + \infty$ along the upper rim of the highest channel. Then the contour would be closing at infinity by means of an almost complete circle, counterclockwise, terminating at the starting point, namely at $+\infty$ on the lower rim of the lowest channel.

Along such a contour, it would be necessary to investigate the behaviors of the ingredients $\mathbf{f}^+$, $\mathbf{W}$ and $\mathbf{\Phi}$ of $\mathbf{G}$. Furthermore, information is needed about the singularities of $\mathbf{G}$ inside the contour; indeed, residues of simple poles are essential for a calculation of $\int dE\, \mathbf{G}(E)$ by Cauchy's theorem; one also needs reasons why no singularities higher than simple poles occur.

The representation discussed in the next subsection makes easier the needed investigation, for it opens two of the cuts and limits the discussion to situations where all momenta have semipositive imaginary parts, $\Im k_j \geq 0$.

B. Pseudomomentum plane

A generalization from [5], where there were two channels only, the present "P representation" consists in joining the upper rim of the lowest cut and the lower rim of the highest cut, and in opening both cuts, by *rational* formulae,

$$k = P + Q^2/P, \quad K = P - Q^2/P, \tag{4}$$

where $Q = e^{i\theta}$ makes a short notation for our scaling of energies such that $E_N^* = 4$ and $k^2 - K^2 = 4Q^2$. Trivially, P is the average $(k + K)/2$ of k and K. The point is, despite an obvious failure to open additional cuts, P also give the "dominant" part of any other momentum when $\Im P \to +\infty$. Indeed, when $|P|$ is large, say $|P| >> 2$, then an asymptotic value can be defined for k_j, $j \neq 1$, $j \neq N$, according to the rule,

$$k_j \equiv (k^2 - Q^2 E_j^*)^{\frac{1}{2}} = (P^2 + 2Q^2 - Q^2 E_j^* + Q^4/P^2)^{\frac{1}{2}} = P + Q^2(1 - E_j^*/2)/P + \mathcal{O}(P^{-2}). \tag{5}$$

Thus the semicircle at infinity in the upper P plane corresponds to $\Im k_j > 0$, $\forall j$. This is of critical value for the zoology of our Jost functions and it is expected that this semicircle properly closes the integration contour under design.

Set now $P = x + iy$ and short notations $c = \cos 2\theta$ and $s = \sin 2\theta$. A trivial calculation separates the real and imaginary parts of the (complex) energies driving each channel,

$$(x^2 + y^2)^2\, \Re(k_j^2) = [(x^2 + y^2 + s)(x + y) + (x - y)c]\,[(x^2 + y^2 - s)(x - y) + (x + y)c] - E_j^*(x^2 + y^2)^2 c, \tag{6}$$

and

$$(x^2 + y^2)^2\, \Im(k_j^2) = 2[(x^2 + y^2)x + xc + ys]\,[(x^2 + y^2)y + xs - yc] - E_j^*(x^2 + y^2)^2 s. \tag{7}$$

and it is trivial to recover the images, in this new representation, of the cuts displayed in Fig. 1. Polar coordinates, with $P = pe^{i\eta}$, can be also be used to decribe the j-th cut from Eq.(7) by,

$$p^2 \sin 2\eta + \frac{\sin(4\theta - 2\eta)}{p^2} = (E_j^* - 2)\, \sin 2\theta. \tag{8}$$

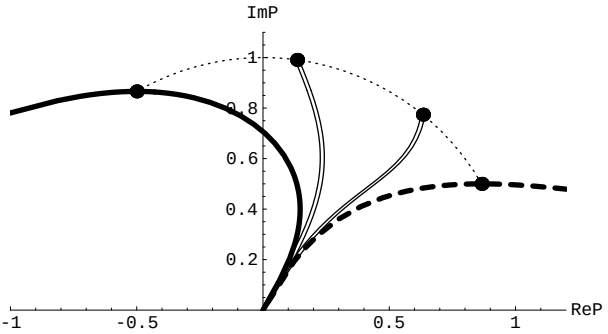

FIG. 2. P plane. Cuts for the same four channel case, $\theta = \pi/6$, $E_2^* = 1.5$, $E_3^* = 3.5$ and $E_4^* = 4$. Opened cut for lowest channel, heavy full line. Opened cut for highest channel, heavy dashed line. Intermediate channel cuts, not open, lighter full lines. The dotted segment is the locus of thresholds (big dots) in this P representation.

Results are shown in Figure 2 for the same special case as Fig. 1. As in [5], the lowest channel is represented by the heavy, shoulder shaped line, that starts from $-\infty$ on the real P axis, bends up, then backs into the origin $P = 0$, where it terminates with a slope 2θ. Along the curve, k is real and runs from $-\infty$ to $+\infty$, covering both rims of the initial cut. The threshold $k = 0$ is represented by $P = iQ = e^{i(\theta+\frac{1}{2}\pi)}$. Partner points where $k \leftrightarrow -k$ obtain under the symmetric transformation $P \leftrightarrow -Q^2/P$. In the same way, for the highest channel, K runs with real values along the heavy dashed line, from $-\infty$ at $P = 0$ to $+\infty$ at the end of the positive $\Re P$ semiaxis, via $K = 0$ for $P = Q$. The transform, $P \leftrightarrow Q^2/P$, makes partners with opposite values of K.

The other cuts remain cuts. Their thresholds lie on the image, shown as a dotted line again, of the segment already pointed out at the stage of Fig. 1. Because both $\Re(k_j^2)$ and $\Im(k_j^2)$ vanish for such points, it is easy to eliminate E_j^* between the right hand sides of Eqs.(6,7) and obtain the condition for such a locus,

$$x^2 + y^2 = 1, \tag{9}$$

a very simple result indeed. With $|P| = 1$, the positions of the thresholds are easy to obtain. The special cases $j = 1$ and $j = N$ give the argument $\eta \equiv ArgP$ as $\eta = \theta + \pi/2$ and $\eta = \theta$, respectively. This was already known from [5]. The function $\sin 2\eta + \sin(4\theta - 2\eta)$, see Eq.(8), decreases monotonically when η increases from θ to $\theta + \pi/2$, hence a unique solution for each E_j^*, and an obvious symmetry about $\theta + \pi/4$ corresponding to the symmetry about $E_j^* = 2$. Then each intermediate cut generates, from Eq.(7), an image which joins its threshold to the origin $P = 0$, while k_j, a real number along this image, runs from 0 to $\pm\infty$, according to the rim. The image lies between the heavy full and dashed lines, and, being pinched between them at $P = 0$, also reaches the origin with slope 2θ. While the pinching makes numerics slightly difficult, it is easy to verify analytically from Eqs.(6,7) that *infinitesimally away from both rims of such an intermediate cut, but inside the wedge created by the heavy line curves, $\Im k_j$ remains positive.*

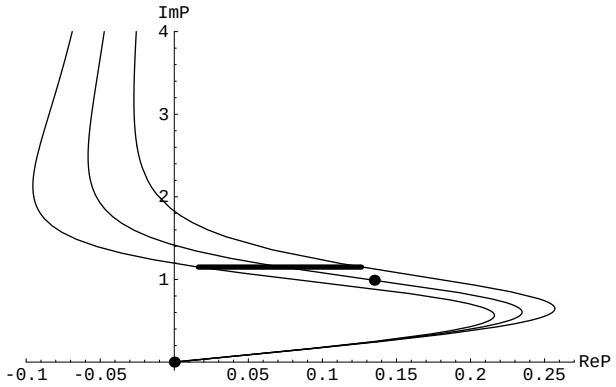

FIG. 3. P plane. Again $\theta = \pi/6$. Cut for the channel defined by $E_2^* = 1.5$. The center line, between dots, is the cut. Cut then continued for negative energies in the channel. Additional lines, lower rim (leftmost curve) and upper rim (rightmost curve), respectively. Both rims extended below threshold. Heavy line bar, connection between extended rims.

To illustrate our full control of the various $\Im k_j$'s provided by this P representation, whether inside the wedge or near the positive infinity semicircle, we show in Figure 3 the cut corresponding to E_2^*, and its continuation beyond threshold. By "beyond", we mean still canceling $\Im k^2$, while $\Re k^2$ becomes more and more negative. This allows reaching the

"semicircle". Simultaneously, we generate rims of the cut, and beyond again below threshold. To generate rims, we use Eq.(7), or as well Eq.(8), with E_2^* replaced by $E_2^* - 0.2$ and $E_2^* + 0.2$ for the lower and upper rim, respectively. (The choice ± 0.2 was made for graphical convenience, but we tested much smaller intervals, naturally.) The dots represent $P = 0$, where the channel energy is infinite, and the threshold, where it vanishes by definition. Like the cut, the rims are pinched by the wedge.

Then we show in Figure 4 the trajectory of k_3 when P follows this cut from $P = 0$, to the threshold and beyond. Notice that, E_2 being real along the line, then the imaginary part of $E_3 = E_2 + e^{2i\theta}(E_2^* - E_3^*)$ is obviously negative. This does not prevent a choice of k_3 with $\Im k_3 > 0$, generating the leftmost trajectory in Fig. 4. Simultaneously, we show the trajectories of k_2 from both rims of the same cut. The left hand side (when seen in Fig. 3) rim induces $\Re k_2 \to -\infty$ when $P \to 0$, with an infinitesimally positive $\Im k_2$. Conversely the right hand side rim induces $\Re k_2 \to +\infty$ when $P \to 0$, with still an infinitesimally positive $\Im k_2$. When we go from either rim towards the upper semicircle at infinity, this induces $\Im k_2 \to +\infty$, as expected. The rims can be connected by any small path, see the bar above the threshold in Fig. 3, and the values of k_2 along the rims can be smoothly matched, see the curved bar in Fig. 4, the trajectory of k_2 when P follows the bar in Fig. 3. Generalizations to every k_j in every part of the wedge are trivial.

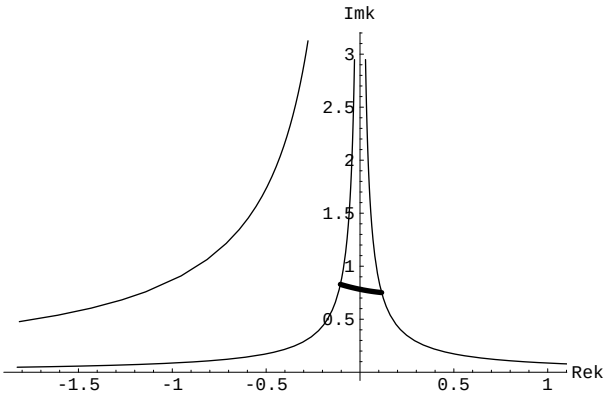

FIG. 4. k_2, k_3 planes. Still $\theta = \pi/6$, $E_2^* = 1.5$ and $E_3^* = 3.5$. Leftmost curve, trajectory of k_3 when P follows the central line of Fig. 3. Intermediate curve, trajectory of k_2 for extended lower rim, see leftmost curve in Fig. 3. Rightmost curve, trajectory of k_2 induced by extended upper rim, see rightmost curve in Fig. 3. Heavy line curved bar, connection trajectory for k_2 when P turns around the threshold, below it.

C. Contour

To synthetize this Section, the P representation defines a physical sheet similar to the physical sheet of the energy plane. The region of interest is that region above the two curves which open the cuts for the lowest and the highest channels, while cuts remain for the intermediate channels. All momenta inside the wedge, and all the way to the upper semicircle at infinity, can be defined with positive imaginary parts. A contour can be found, following all cuts and closing at infinity in the upper plane.

The intuition which was present in the E representation can be substantiated in the P plane. Start from $-\infty$ on the

real axis, follow the "opener curve" which corresponds to the lowest channel, all the way to $P = 0$. From there, follow the lower rim of the cut corresponding to the second channel, back to its threshold, then turn around the threshold to follow its upper rim, down to $P = 0$. In turn, follow the lower rim of each intermediate channel, then its upper rim. After bouncing $N - 1$ times at $P = 0$, follow the "opener curve" corresponding to the upper channel, until $P \to +\infty$ on the real axis. Then close the contour by means of the upper semicircle at infinity. In the next Section, we shall investigate what happens to the integral, $\mathcal{I} = \int dE\, \mathbf{G}(E, r, r')$, when considered along this contour in the P plane.

III. THREE CONTRIBUTIONS TO THE GREEN'S FUNCTION INTEGRAL

A. Upper semicircle

At infinity in this upper P plane, the integration weight, $dE = 2\left(P - Q^4/P^3\right) dP$, boils down to $2P\, dP$. All the N distinct Jost solutions boil down to $\exp\left[i(Pr - \frac{1}{2}\ell_j\pi)\right]$ in their respective "flux channel j", while vanishing in the other channels. At the same time, the N distinct regular solutions similarly boil down to $\sin\left(Pr - \frac{1}{2}\ell_j\pi\right)/P$ in their respective flux channel and vanish in the other channels. The Wronskian matrix boils down to the N-dimensional unit matrix.

Assume now $r > r'$, for instance, and thus consider the second of Eqs.(3). The product $\mathbf{f}^+ [\tilde{\mathbf{W}}]^{-1} \tilde{\mathbf{\Phi}}$ boils down to a diagonal matrix. Its j-th diagonal element reads,

$$\int_{sc} 2\, dP\; e^{i(Pr - \ell_j\pi/2)}\, \sin\left(Pr' - \ell_j \frac{\pi}{2}\right), \tag{10}$$

and can be easily calculated by reducing the semicircle back to the real P axis. The result does not depend on j,

$$-i \int_{\infty}^{-\infty} dP\, e^{i(Pr - \frac{1}{2}\ell_j\pi)} \left[\exp\left(iPr' - i\ell_j \frac{\pi}{2}\right) - \exp\left(i\ell_j \frac{\pi}{2} - iPr'\right)\right] = 2i\pi[\delta(r + r') - \delta(r - r')]. \tag{11}$$

It is trivial to verify that the same result is obtained if $r < r'$. Furthermore the term $\delta(r + r')$ cancels out in the space of regular radial waves. Hence the contribution $\mathcal{I}_{sc}$ of the semicircle makes nothing but the multichannel identity, multiplied by $(-2i\pi)$. Notice that, differing from [2], this identity is not multiplied by a factor depending on θ, since for us the ends of the semicircle, $-\infty$ and $+\infty$, both lie on the real P axis.

B. Continuum

It makes no difference here whether we consider the contribution of one of the "opener line" or that of one of the intermediate cuts. For in both cases we group partner terms. Such partners either come from a transform $P \leftrightarrow \pm Q^2/P$ or from opposite rims of the intermediate cut under consideration. What is important to notice is that momenta retain their finite and positive imaginary parts and do not change when we compare two partner points, except that momentum specific to the opener line or the cut. For that momentum, which is real, "partnership" means $k_j \leftrightarrow -k_j$, with still an infinitesimal positive imaginary part. Keeping in mind that $\mathbf{\Phi}$ is even under such a momentum flip, the contribution of such a continuum thus reads, if $r > r'$ for instance,

$$\mathcal{I}_j = \int_0^{\infty} 2k_j\, dk_j\, \mathbf{D}_j(E, r)\, \tilde{\mathbf{\Phi}}(E, r'), \tag{12}$$

where $\mathbf{D}_j(E, r)$ represents the following difference between partners,

$$\mathbf{D}_j(E, r) = \mathbf{f}^+(E, r)\, [\tilde{\mathbf{W}}(E)]^{-1} - \mathbf{f}^+(-k_j, r)\, [\tilde{\mathbf{W}}(-k_j)]^{-1}, \tag{13}$$

a discontinuity across the cut. The notation used here takes advantage of the fact that $dE = 2k_j dk_j$, and that k_j is a convenient label along the line or the cut. The first term, $\mathbf{f}^+(E, r)\, [\tilde{\mathbf{W}}(E)]^{-1}$, in the right hand side of Eq.(13) clearly comes from the upper rim. The notation that we use for the second term, $\mathbf{f}^+(-k_j, r)\, [\tilde{\mathbf{W}}(-k_j)]^{-1}$, indicates that, because of analytic continuation in the physical sheet around the threshold, one Jost solution $f^-_{\cdot j}$ now makes the j-th column of $\mathbf{f}$ and that of $\tilde{\mathbf{W}}$. *All other columns are unchanged, and this strong similarity reduces the difference* $\mathbf{D}_j$ *to*

be a rank one dyadic. An elementary proof of this dyadic result was given in Appendix C of [5]. Nothing changes in the argument if $r < r'$.

As a consequence of the dyadic nature of $\mathbf{D}_j$, and of the symmetry $\mathbf{G}(E,r,r') = \mathbf{G}(E,r',r)$, hence of the same symmetry for discontinuities across cuts, there exists as a column vector a solution $\phi_{.j}$ of Eqs.(1) that is able to represent symmetrically both $\mathbf{D}_j(E,r)\,\tilde{\mathbf{\Phi}}(E,r')$ and $\mathbf{\Phi}(E,r)\,\tilde{\mathbf{D}}_j(E,r')$ in a self dual way as an outer product,

$$\mathcal{I}_j = \int_0^\infty 2k_j\,dk_j\,\frac{\phi_{.j}(E,r)\,\tilde{\phi}_{.j}(E,r')}{\mathcal{D}(E)}. \tag{14}$$

This solution belongs to the set of regular solutions, naturally, because of the regularity of $\mathbf{G}$ at both $r = 0$, and $r' = 0$, illustrated by the presence of $\mathbf{\Phi}$ in Eqs.(3). The exact natures of this $\phi_{.j}$ and of the "normalizing" denominator $\mathcal{D}$ are discussed in the Appendix.

At this stage, the full integral along the full contour thus gives the sum of the multichannel identity and "pseudo-projectors on the continuum", one pseudoprojector for each channel,

$$\frac{i}{2\pi}\int dE\,\mathbf{G}(E,r,r') = \begin{bmatrix} \delta(r-r') & 0 & ... & 0 \\ 0 & \delta(r-r') & ... & 0 \\ . & . & . & . \\ 0 & 0 & ... & \delta(r-r') \end{bmatrix} + \frac{i}{\pi}\sum_{j=1}^{N}\int_0^\infty k_j\,dk_j\,\frac{\phi_{.j}(E,r)\,\tilde{\phi}_{.j}(E,r')}{\mathcal{D}(E)}. \tag{15}$$

The next subsection shows what happens if the same integral is evaluated by means of the Cauchy theorem.

C. Residues at poles

We assumed that, before complex scaling, namely for $\theta = 0$, there existed an identity resolution in terms of unscaled bound states and unscaled scattering states. In other words we assumed that the corresponding, unscaled $\mathbf{G}(E)$ shows only isolated, simple poles, besides the physical cuts. Such poles can be on the real E axis of the physical sheet, describing bound states, or away from this axis, then describing resonances or antiresonances. The point is, now, that the CSM cannot change the nature of such poles [1]. Within our description by Eqs.(1), the CSM just rotates such poles by 2θ in the energy representation, along circular arcs, concentric around $E = 0$. In the P representation, the images of such arcs are also concentric arcs, with angular extension θ only. This is trivially seen from the equation which, for each initial position ε of a pole, defines those values of P which represent $e^{2i\theta}\varepsilon$,

$$\left(P + e^{2i\theta}/P\right)^2 = e^{2i\theta}\,\varepsilon. \tag{16}$$

Indeed, θ disappears from this equation if one sets $P = e^{i\theta}P_0$, where P_0 solves for the initial position ε. It can be concluded that only simple poles will be found when a finite θ is used for our CSM. Notice, incidentally, that for ε real and negative (bound states), the P representation will align poles along the axis with polar angle $\theta + \pi/2$, further than the circle with radius 1 that we found as the locus of thresholds. There will be no such alignment for resonances.

For the calculation of $\mathcal{I}$ by Cauchy's theorem, poles are not due to either $\mathbf{f}$ or $\mathbf{\Phi}$, since these, as functions of E or P, are regular. Only the divergence of $\mathbf{W}^{-1}$ can create poles. The situations of interest are those when the roots of the determinant, $\det\mathbf{W}$, are located inside the integration contour. We know that such is the case for the bound states. Depending upon θ, some resonances may also rotate into the domain. It is already known that only simple, isolated poles occur. The only question to solve is, what is the residue of $\mathbf{G}$ at such a pole.

Residues of $\mathbf{G}$ at its poles will now be obtained from derivatives d/dE. That is equivalent to a calculation in the P representation, anyhow, and slighly easier. We shall use short notations in which the dependence of $\mathbf{\Phi}$, $\mathbf{f}^+$, $\mathbf{W}$, upon r, and/or r' and/or E will be most often understood. However, at those energies E_ν where a pole occurs, we use an explicit subscript ν to specify that such quantities $\mathbf{\Phi}$, ... , $\mathbf{W}$ are evaluated at E_ν.

Poles occur because of $\mathbf{W}^{-1}$. Hence, we must only find the residue,

$$\mathcal{R}_\nu = \lim_{E\to E_\nu}\,(E - E_\nu)\;\mathbf{W}^{-1}(E)\,, \tag{17}$$

and form the matrix product $\mathbf{\Phi}\,\mathcal{R}_\nu\,\tilde{\mathbf{f}}^+$ and its transpose $\mathbf{f}^+\tilde{\mathcal{R}}_\nu\,\tilde{\mathbf{\Phi}}$.

At a (simple!) root E_ν of $\det \mathbf{W}(E)$, there is necessarily one, and just one, null right eigenvector Λ_ν of $\mathbf{W}$. Similarly there is one, and just one, null left eigenvector Λ'_ν. We write them as columns and normalize them by the condition,

$$\tilde{\Lambda}'_\nu \, \Lambda_\nu = 1. \tag{18}$$

Then the divergent part of $\mathbf{W}^{-1}$ in a neighborhood of E_ν is nothing but the truncation,

$$\mathbf{W}^{-1}_{tr} = \frac{\Lambda_\nu \, \tilde{\Lambda}'_\nu}{\tilde{\Lambda}'_\nu \, \mathbf{W}(E) \, \Lambda_\nu} \,, \tag{19}$$

where there is an explicit dependence on E in the denominator. This denominator, a number, vanishes at $E = E_\nu$. As a matrix element of $\mathbf{W}$ it is nothing but the Wronskian of the following two waves, $F \equiv \mathbf{f}^+ \, \Lambda'_\nu$ and $\xi \equiv \Phi \, \Lambda_\nu$. The former, F, is irregular, the latter, ξ, is regular. While Λ_ν and Λ'_ν do not depend on E, since they were defined at $E = E_\nu$, both F and ξ depend on E, via $\mathbf{f}^+$ and $\mathbf{\Phi}$. When their Wronskian vanishes, F and ξ become proportional to each other, and there exits a number c such that $F_\nu = c \, \xi_\nu$. This special wave is both a mixture of regular solutions and a mixture of Jost solutions, with positive imaginary parts in the momenta driving all Jost solutions. Therefore it decreases exponentially in all channels when $r \to \infty$ and it is square integrable as well as regular. As expected it represents either a bound state or a regularized resonance.

According to Eqs.(17,19), the residue under study comes from just the reciprocal of the derivative of the Wronskian of F and ξ,

$$\mathcal{R}_\nu = \frac{\Lambda_\nu \, \tilde{\Lambda}'_\nu}{d \left[\tilde{\Lambda}'_\nu \, \mathbf{W}(E) \, \Lambda_\nu \right] / dE \, |_{E=E_\nu}} \,. \tag{20}$$

In short, we must calculate the derivative of a Wronskian with respect to the energy, $d \left[\tilde{\Lambda}'_\nu \, \mathbf{W}(E) \, \Lambda_\nu \right] / dE$. To help manipulations with Wronskians, define an operator matrix $\mathbf{U}$ with matrix elements the CSM potentials, completed by the centrifugal barriers and the thresholds,

$$\mathbf{U}_{ij} = e^{2i\theta} U_{ij} \left(e^{i\theta} r \right) + \delta_{ij} \left[e^{2i\theta} E_j^* + \frac{\ell_j (\ell_j + 1)}{r^2} \right]. \tag{21}$$

Then elementary, but slightly tedious manipulations, which are already described in [10] or in Appendix B of [5], give the remarquably simple result,

$$d \left[\tilde{\Lambda}'_\nu \, \mathbf{W}(E) \, \Lambda_\nu \right] / dE \, |_{E=E_\nu} = - \, c \int_0^\infty dr \, \tilde{\xi}(E_\nu, r) \, \xi(E_\nu, r). \tag{22}$$

Then the constant c cancels out between this and the numerators of $\mathbf{f}^+_\nu \, \tilde{\mathcal{R}}_\nu \, \tilde{\mathbf{\Phi}}_\nu$ and $\mathbf{\Phi}_\nu \, \mathcal{R}_\nu \, \tilde{\mathbf{f}}^+_\nu$, which make the same, symmetric formula anyway, whether $r > r'$ or $r < r'$, since $F_\nu = c \, \xi_\nu$.

Summing upon all such residues obtained at roots E_ν of $\det \mathbf{W}$ above the "opener" curves in the P upper half-plane, the contour integral reads,

$$\mathcal{I}(r, r') = - \, 2 \, i \, \pi \sum_\nu \, \frac{\mathbf{\Phi}(E_\nu, r) \; \Lambda_\nu \; \tilde{\Lambda}_\nu \; \tilde{\mathbf{\Phi}}(E_\nu, r')}{\int_0^\infty dr'' \, \tilde{\Lambda}_\nu \; \tilde{\mathbf{\Phi}}(E_\nu, r'') \; \mathbf{\Phi}(E_\nu, r'') \; \Lambda_\nu} \,. \tag{23}$$

Here we state again that the column vector Λ_ν is the null, right-hand side eigenvector of $\mathbf{W}(E_\nu)$, namely $\mathbf{W}(E_\nu) \, \Lambda_\nu = 0$, then the column vector $\mathbf{\Phi}(E_\nu) \, \Lambda_\nu$ of wave functions is the wave function of the bound state or resonance, and the denominator plays the role of a "Euclidean-like square norm". This denominator is non vanishing; this corresponds to the hypothesis of single, isolated poles. All these are labeled by ν, a discrete index, or as well by P_ν, an isolated root of $\mathbf{W}$ if viewed as a function of P.

D. Completeness

Since the three contributions $\mathcal{I}_{sc}$, $\sum_j \mathcal{I}_j$ and $\mathcal{I}$ are obviously related by $\mathcal{I}_{sc} + \sum_j \mathcal{I}_j = \mathcal{I}$, it is trivial to equate $\frac{i}{2\pi} \mathcal{I}_{sc}$, the multichannel identity, with the difference between $\frac{i}{2\pi} \mathcal{I}$, the pseudoprojector on both bound states and resonances,

and $\frac{i}{2\pi}\sum_j \mathcal{I}_j$, the latter term making the pseudoprojector upon the continuum for all channels. Naturally, in practical calculations, a cutoff and some amount of discretization will be necessary to integrate such continuum terms, but the P representation provides a suitable frame for testing the convergence of such a resolution for sum rules, level densities and similar observables. Notice that, because of the use of complex, self dual bras and kets in the resolution, such cutoff and discretization manipulations may generate spurious imaginary parts for the expectation values of hermitian observables. For a discussion and possible interpretation of imaginary parts in individual matrix elements, we refer to [11]. But, when summed upon all discrete and integral terms provided by the resolution, such imaginary parts must add up to a negligible, spurious noise compared to the real parts. This requested cancellation makes one more criterion to validate numerical operations.

IV. DISCUSSION AND CONCLUSION

Once again we used the ABC theorems [1] to locate the discrete spectrum at trivially rotated positions deduced from the discrete spectrum of an initial, hermitian Hamiltonian. The topological similitude provided by the CSM rotation warrants that, as long as there are no double poles or higher singularities with the initial Hamiltonian, the same will be true with the CSM Hamiltonian.

Then it was not very difficult to find a representation which allows a suitable contour integration of the Green's function. There was still a slightly complicated Riemann surface to handle, for the number of cuts was reduced to $N-2$ only [12], but we took great care, including a few numerical, illustrative examples, to show that all cuts in the new representation are well understood, all thresholds are easily located, all complex momenta to be used for proofs have positive imaginary parts in a physical domain of a suitable sheet, and in general that all technicalities are sound.

This proof of the CSM completeness for N channels is restricted to a finite number of well separated channels, normal square root threshold singularities, in a purely inelastic situation, without rearrangement, and with short ranged forces. The case of long range forces makes a more difficult question, indeed [13] [14]. But our restrictions still allow a large class of practical problems, and for instance in nuclear physics, a very large number of collective resonances can be described by the coupled channel equations that we studied.

Acknowledgment: B.G.G. thanks the Hokkaido University for its hospitality during part of this work.

---

[1] Aguilar, J. and Combes, J.M. *Commun. Math. Phys.* **22** (1971) 269; Aguilar, J. and Balslev, E. *Commun. Math. Phys.* **22** (1971) 280

[2] Myo, T. Ohnishi, A. and Katō, K. *Progr. Th. Phys.* **99** (1998) 801

[3] Myo, T., Katō, K., Aoyama, S. and Ikeda, K. *Phys. Rev. C* **63** (2001) 054313-1

[4] Berggren, T. *Phys. Lett.* **B44** (1973) 23; Romo, W. J. *Nucl. Phys.* **A237** (1975) 275

[5] Giraud, B.G. and Katø, K. *Ann. Phys.* **308** (2003) 115

[6] Krylov, N.S. and Fock, V.A. *Zh. Eksp. Teor. Fiz.* **17** (1947) 93; Fonda, L., Ghirardi, G.C. and Rimini, A. *Rep. Prog. Phys.* **41** (1978) 587

[7] Menon, V.J. and Lagu, A.V. *Phys. Rev. Lett.* **51** (1983) 1407

[8] Barrett, R.F., Robson, B.A. and Tobocman, W. *Rev. Mod. Phys.* **55** (1983) 155

[9] Robson, D. pp. 179-248 in *Nuclear Spectroscopy and Reactions*, J.Cerny ed., Academic Press N.Y. and London (1975)

[10] Newton, R.G. *Scattering Theory of Waves and Particles* (1982) Springer Verlag (New-York, Heidelberg, Berlin) ISBN 0-387-10950-1, 3-540-10950-1; see in particular chapters 12, 15 and 17.

[11] Berggren, T. *Phys. Lett.* **B373** (1996) 1

[12] Weidenmüller, H.A., *Ann. of Phys.* **28** (1964) 60

[13] Ho, Y.K. *Phys. Reports* **99** (1983) 1; see also the reference list of this paper

[14] Moiseyev, N. *Phys. Reports* **302** (1998) 211; see also the reference lists of this paper

Appendix

We give here in some detail a description of that regular solution $\phi_{.j}$ which accounts for the discontinuity of the Green's function across a cut. For the sake of pedagogy, we set the channel number to be $N = 4$ and shall consider only what happens for, e.g., the second cut. Generalizations are obvious and left as an exercise for the interested reader. In a condensed notation, we write the upper rim Wronskian matrix as,

$$\mathbf{W}_u = \begin{bmatrix} a & b & c & d \\ e & f & g & h \\ i & j & k & l \\ m & n & o & p \end{bmatrix}. \tag{24}$$

where, for instance, b is the Wronskian of $f^+_{.1}$ with $\varphi_{.2}$ and o is the Wronskian of $f^+_{.4}$ with $\varphi_{.3}$. The inverse of $\mathbf{W}_u$ reads, trivially,

$$\mathbf{W}_u^{-1} = (det_u)^{-1} \begin{bmatrix} a' & e' & i' & m' \\ b' & f' & j' & n' \\ c' & g' & k' & o' \\ d' & h' & l' & p' \end{bmatrix}, \tag{25}$$

where det_u is the determinant of $\mathbf{W}_u$ and the prime symbols denote the corresponding cofactors. For the lower rim of the second cut a substitution occurs for the second row of $\mathbf{W}_u$, hence the lower rim Wronskian matrix reads,

$$\mathbf{W}_l = \begin{bmatrix} a & b & c & d \\ q & r & s & t \\ i & j & k & l \\ m & n & o & p \end{bmatrix}, \tag{26}$$

where, for instance, t is the Wronskian of $f^-_{.2}$ with $\varphi_{.4}$. Accordingly the inverse matrix becomes,

$$\mathbf{W}_l^{-1} = (det_l)^{-1} \begin{bmatrix} a'' & e' & i'' & m'' \\ b'' & f' & j'' & n'' \\ c'' & g' & k'' & o'' \\ d'' & h' & l'' & p'' \end{bmatrix}, \tag{27}$$

where doubleprime symbols denote new cofactors, but the cofactors of $\{q, r, s, t\}$ are the same as those of $\{e, f, g, h\}$.

Again with a transparent, condensed notation, we set, for the upper and lower rim, respectively,

$$\tilde{\mathbf{f}}^u = \begin{bmatrix} A & B & C & D \\ E & F & G & H \\ I & J & K & L \\ M & N & O & P \end{bmatrix}, \quad \tilde{\mathbf{f}}^l = \begin{bmatrix} A & B & C & D \\ Q & R & S & T \\ I & J & K & L \\ M & N & O & P \end{bmatrix}. \tag{28}$$

with, for instance, $\{A, B, C, D\} \equiv \{f^+_{11}, f^+_{21}, f^+_{31}, f^+_{41}\}$, and $\{E, F, G, H\} \equiv \{f^+_{12}, f^+_{22}, f^+_{32}, f^+_{42}\}$, while $\{Q, R, S, T\} \equiv \{f^-_{12}, f^-_{22}, f^-_{32}, f^-_{42}\}$. For $r < r'$, the discontinuity to be studied corresponds to the transposed of Eq.(13), and reads, in a condensed notation,

$$\tilde{\mathbf{D}}_2(r') = \mathbf{W}_u^{-1}\, \tilde{\mathbf{f}}^u(r') - \mathbf{W}_l^{-1}\, \tilde{\mathbf{f}}^l(r'), \tag{29}$$

The subscript 2 for the cut and the r' dependence will be now understood and we shall use trivial identities to analyze

$$\tilde{\mathbf{D}} = \left[\mathbf{W}_l^{-1} + \mathbf{W}_l^{-1}\,(\Delta\mathbf{W})\,\mathbf{W}_u^{-1}\right]\,\tilde{\mathbf{f}}^u - \mathbf{W}_l^{-1}\,(\tilde{\mathbf{f}}^u + \Delta\tilde{\mathbf{f}}) = \mathbf{W}_l^{-1}\,(\Delta\mathbf{W})\,\mathbf{W}_u^{-1}\,\tilde{\mathbf{f}}^u - \mathbf{W}_l^{-1}\,\Delta\tilde{\mathbf{f}}, \tag{30}$$

where $\Delta\mathbf{W} = \mathbf{W}_l - \mathbf{W}_u$ and $\Delta\tilde{\mathbf{f}} = \tilde{\mathbf{f}}^l - \tilde{\mathbf{f}}^u$. The point is, both modifications Δ are just substitutions for second rows; they boil down to dyadics,

$$\Delta\mathbf{W} = \begin{bmatrix} 0 \\ 1 \\ 0 \\ 0 \end{bmatrix} \otimes \begin{bmatrix} q-e & r-f & s-g & t-h \end{bmatrix}, \qquad \Delta\tilde{\mathbf{f}} = \begin{bmatrix} 0 \\ 1 \\ 0 \\ 0 \end{bmatrix} \otimes \begin{bmatrix} Q-E & R-F & S-G & T-H \end{bmatrix}. \tag{31}$$

(Our use of the tensor product symbol $\otimes$ is actually superfluous; we just want to stress the matrix product of a column by a row.) The next point is, then, that a global dyadic form for $\tilde{\mathbf{D}}$ emerges,

$$\tilde{\mathbf{D}} = \mathbf{W}_l^{-1} \begin{bmatrix} 0 \\ 1 \\ 0 \\ 0 \end{bmatrix} \otimes \Big(\begin{bmatrix} q-e & r-f & s-g & t-h \end{bmatrix} \mathbf{W}_u^{-1} \tilde{\mathbf{f}}^u - \begin{bmatrix} Q-E & R-F & S-G & T-H \end{bmatrix} \Big). \tag{32}$$

Furthermore, from the very definition of matrix inversion, we see that

$$\begin{bmatrix} e & f & g & h \end{bmatrix} \mathbf{W}_u^{-1} = \begin{bmatrix} 0 & 1 & 0 & 0 \end{bmatrix}, \tag{33}$$

hence

$$\begin{bmatrix} -e & -f & -g & -h \end{bmatrix} \mathbf{W}_u^{-1} \tilde{\mathbf{f}}^u = -\begin{bmatrix} E & F & G & H \end{bmatrix}, \tag{34}$$

and $\tilde{\mathbf{D}}$ simplifies into

$$\tilde{\mathbf{D}} = (det_l)^{-1} \begin{bmatrix} e' \\ f' \\ g' \\ h' \end{bmatrix} \otimes \Big(\begin{bmatrix} q & r & s & t \end{bmatrix} \mathbf{W}_u^{-1} \tilde{\mathbf{f}}^u - \begin{bmatrix} Q & R & S & T \end{bmatrix} \Big). \tag{35}$$

For $r < r'$ the complete discontinuity $\mathbf{\Phi}(r)\, \tilde{\mathbf{D}}(r')$ of $\mathbf{G}(r, r')$ thus reads

$$det_l\ det_u\ \mathbf{\Phi}(r)\ \tilde{\mathbf{D}}(r') = \phi(r)\, \tilde{\Xi}(r'), \tag{36}$$

with

$$\phi = e'\, \varphi_{.1} + f'\, \varphi_{.2} + g'\, \varphi_{.3} + h'\, \varphi_{.4}, \tag{37}$$

and

$$\Xi = (qa' + rb' + sc' + td')\, f_{.1}^{+} + (qe' + rf' + sg' + th')\, f_{.2}^{+} + \ \ldots\ + (qm' + rn' + so' + tp')\, f_{.4}^{+} - det_u\, f_{.2}^{-}. \tag{38}$$

Both ϕ and Ξ are column vectors and relate to the second cut, hence they should actually read $\phi_{.2}$ and $\Xi_{.2}$ in a notation compatible with Eqs.(14,15). We omitted such subscripts, for the sake of conciseness.

It may be convenient to take advantage of the cofactor nature of all the coefficients a', ... p'. This gives indeed the formal, but condensed formula,

$$\phi = \det \begin{bmatrix} a & b & c & d \\ \varphi_{.1} & \varphi_{.2} & \varphi_{.3} & \varphi_{.4} \\ i & j & k & l \\ m & n & o & p \end{bmatrix}. \tag{39}$$

Similarly, we find the formal result,

$$\Xi = -\det \begin{bmatrix} a & b & c & d & f_{.1}^{+} \\ e & f & g & h & f_{.2}^{+} \\ i & j & k & l & f_{.3}^{+} \\ m & n & o & p & f_{.4}^{+} \\ q & r & s & t & f_{.2}^{-} \end{bmatrix}, \tag{40}$$

because all coefficients such as,

$$qa' + rb' + sc' + td' = \det \begin{bmatrix} q & r & s & t \\ e & f & g & h \\ i & j & k & l \\ m & n & o & p \end{bmatrix}, \ \ \ldots\ \ , \ \ qm' + rn' + so' + tp' = \det \begin{bmatrix} a & b & c & d \\ e & f & g & h \\ i & j & k & l \\ q & r & s & t \end{bmatrix}, \tag{41}$$

can themselves be interpreted, after keeping track of signs, as cofactors for the last column of the determinant shown by Eq.(40).

In the $2N$-dimensional space of solutions, it is known that the $2N$ Jost solutions and the N regular ones are related by a formula such as,

$$\mathbf{f}^- = \mathbf{\Phi}\,\mathbf{W}^{-1}\,\mathbf{w} + \mathbf{f}^+\,\mathbf{w}^{-1}\,\mathbf{W}_-\,\mathbf{W}^{-1}\,\mathbf{w}, \tag{42}$$

where $\mathbf{W}$ is the same as $\mathbf{W}_u$, while $\mathbf{W}_-$ is the analog of $\mathbf{W}$ if one replaces each $f^+_{.m}$ by its partner $f^-_{.m}$. Then $\mathbf{w}$ is a diagonal matrix, defined from the Wronskians $\mathcal{W}\,(f^+_{.m}, f^-_{.n}) = -2ik_m\delta_{mn}$. It will be noticed from Eq.(42) that, if we expand an $f^-_{.m}$ on the basis spanned by all the $\varphi_{.n}$ and all the $f^+_{.n}$, the regular components of $f^-_{.m}$ are provided by the m-th column of the matrix product $\mathbf{W}^{-1}\,\mathbf{w}$.

It is known that Ξ always belongs to the subspace of N regular solutions. In our illustrative example where $N = 4$ and we studied the second cut, our Ξ, according to Eq.(38), is a superposition of five solutions, namely all the $f^+_{.n}$ and one $f^-_{.n}$ only, $f^-_{.2}$. After an expansion of $f^-_{.2}$ on the basis spanned by the $\varphi_{.n}$ and the $f^+_{.n}$, all its irregular components must cancel out those preexisting irregular components of Ξ seen from Eq.(38). (For the sake of rigor, we verified, by brute force calculations when $N = 2$, 3 and 4, that the components $f^+_{.n}$ do vanish out.) Thus we may consider the regular components only, coming from just $f^-_{.2}$.

The weight of $f^-_{.2}$ is, according to Eq.(38), $-det_u$. We must therefore find the second column of,

$$-det_u\,\mathbf{W}^{-1}\,\mathbf{w} = -\begin{bmatrix} a' & e' & i' & m' \\ b' & f' & j' & n' \\ c' & g' & k' & o' \\ d' & h' & l' & p' \end{bmatrix}\begin{bmatrix} -2ik_1 & 0 & 0 & 0 \\ 0 & -2ik_2 & 0 & 0 \\ 0 & 0 & -2ik_3 & 0 \\ 0 & 0 & 0 & -2ik_4 \end{bmatrix}, \tag{43}$$

hence the final result,

$$\Xi = 2ik_2\,(e'\,\varphi_{.1} + f'\,\varphi_{.2} + g'\,\varphi_{.3} + h'\varphi_{.4}) = 2ik_2\,\phi. \tag{44}$$

The generalization, $\Xi_{.j} = 2ik_j\,\phi_{.j}$ is obvious. For any channel number N and any j-th cut, both ϕ and Ξ correspond to the j-th column of $\mathbf{W}^{-1}$, hence to the cofactors of the j-th row of $\mathbf{W}$. There is no need here to specify $\mathbf{W}_u$ or $\mathbf{W}_l$, because the relevant cofactors are the same on both rims of the cut. The fact that Ξ and ϕ are the same except for the factor $2ik_j$ gives the same, symmetrical result whether r is larger or smaller than r'. And the denominator present in Eqs.(14,15) reads, when all factors are collected,

$$\mathcal{D}(E) = \frac{det_u\,det_l}{2ik_j}\,. \tag{45}$$